Non-Flow-Pattern Dependent Method Study For Velocity Profile Estimation Using A Electrical Capacitance Tomography

V. Mosorov, D. Sankowski

Computer Engineering Department, Technical University of Łódź,18/22 Stefanowskiego, 90-924 Lodz, Poland mosorow[dsan]@kis.p.lodz.pl

Reviewer: M. Takei (Nihon University, Japan)

Summary: This paper presents an study of the non-flow-pattern dependent method permitting a solid velocity field to be unambiguously calculated with higher robust using a twin-plane electrical capacitance system. It is based on a spectrum analysis of the pixel values of both cross-sections of the tomographic system. The numerical results of flow velocity measurement using the proposed method against the correlation method are presented.

Keywords: electrical capacitance tomography, flow velocity, "virtual tracer"

1. Introduction

Modern flowmeters enable us to evaluate how much material has passed through the meter in a certain time (for example kilograms per hour). For single flows, the technology to measure the flow is well understood and flowmeters are widespread. However, many industrial processes use multiphase flows pumped along pipes. The measurement of the multiphase flow of gas, oil, and water is not trivial (Williams Beck, 1995) and significant challenges include:

- the reduction of multiphase flow measurement uncertainties which depends on the measurement conditions;
- making the flow meters less sensitive to changes in the physical properties of the flow components;
- the improvement of stability over time;
- the reduction of the flow regime dependency for the multiphase flow meters.
- Electrical Tomography (ET) is a typical completely non-intrusive technique for measuring multiphase flow in pipes. This technique can be used for measuring different kinds of multiphase flows such as gas/solids (Jaworski, Dyakowski 2001), gas/liquid (Fehmers, 2003), and liquid/solids flows.

There exist two widely applied types of ET tomography: Electrical Resistance Tomography (ERT) and Electrical Capacitance Tomography (ECT). Currently more papers about flow measurement using ECT (Byars et al., 2003) and ERT systems (Bolton el al., 2003) have been published.

The flowmeter for measuring the flow rate based on Electrical Capacitance Tomography technique consists of two separate planes of sensors, which measure electrical capacitance between two pairs of electrodes around a pipe.

To calculate the cross sectional distribution of the permittivity of the material (or concentration profiles) inside the pipe from the capacitance measurements an image reconstruction algorithm is used. The images provide instantaneous information on material distribution in the two pipe cross-sections at given locations. With the sensor dimensions we can then calculate the volume flow rate per zone. As result, the integration of the volumetric flow, if the density is known, mass flow can be derived.

Although acquisition and processing were initially seriously limited by computing speed, the commercial ECT systems, which are now available, can produce twin-plane images with real-time image capture and reconstruction at up to 300 complete frames per second (Hunt, 2003). Such systems include major commercial applications such as pneumatic conveying of solids, many flow mixtures within the oil industry, and gas-solid fluidized beds (Byars et al, 2003; Corlett, 2001).

However, technological progress needs to focus on developing new theoretical approaches, which would permit the measurement of flow parameters more accurately and reliably.

2. Methods for flow velocity calculation in Tomography image Velocimetries - Review

The solids motion has a stochastic character and hence typical solid concentration changes within any pixel of two cross-sections can be treated as stochastic stationary process.

Let $x_n(iT)$ and $y_n(iT)$, n=0,...,N-1, where N is the total number of image pixels, define instantaneous distributions of material for the nth pixel of the ith image obtained from the cross-sections X and Y respectively within the frame rate resolution T *(*frame *per second)*. Nowadays, there exist two methods to calculate the transit time τ of flow propagation from reconstructed images of two planes: classical correlation method (Beck, 1981) and weighted-mean phases method (Mosorov, 2006).

These methods for calculating velocity are based on two main assumptions:

1. The trajectories of motion between these sensors are parallel to the pipe axis (the trajectories are perpendicular to the sensor plane),
2. The changes within any pixel of a pipe cross-section are treated as a stationary or quasi-stationary process and hence the correlation function $R_{xy}(\tau)$ describes the general dependence between any process from the first plane and another from the second plane.

As discussed in the literature (Beck, 1981), the particle transition time τ can be found by cross-correlating corresponding processes $x_n(t)$ and $y_n(t)$. For

the reconstructed images obtained within the frame rate T the cross correlation can be calculated as following:

$$R_{x_n y_n}(pT) = \frac{1}{M}\sum_{i=0}^{M-1} x_n(iT)\, y_n((i+p)T), \qquad (1)$$

where p = ..., -1, 0, 1, ... is the shift time in the number of frames; n is the pixel index, M is the number of images for which the cross-correlation is calculated; $x_n(iT)$, $y_n(iT)$ are the numerical values, associated with pixel n from i image obtained from sensors of a plane X and plane Y, respectively, T is time period of a single frame.

In the simplest assumption the shift p_τ at the peak of the correlogram corresponds to a transit time τ of flow structures between two planes, $\tau_x = p_\tau \cdot T$. Knowledge of the transit time τ and distance d between the two sensors enables the solids velocity within nth pixel to be calculated from the following equation (2):

$$v_n = d/\tau = d/p_\tau \cdot T \qquad (2)$$

In total, N velocities, which have created a velocity profile, can be calculated [vn], n=0,…,N-1.

Another aspect to consider is what the velocity v (eq.1) we thus measure? Since transit time τx is calculated at a time interval, therefore this velocity cannot be a temporary velocity of material propagation between two planes of the sensors.

The calculated correlogram has a clearly discernible peak if the flow patterns take a form similar a rectangular impulse (such as flow instabilities referred to as “slugs” and “plugs” in the dense pneumatic conveying transport) over the correlation interval. Consequently, the flow regime (stratified, slug, annular or bubble flow and flow direction) has significant influence for finding a correlogram peak.

The peak may be found by the greatest single value, centre of area or polynomial fitting. The polynomial fitting gives the most consistent results though all the other techniques are available in the software.

Although cross-correlation technique has many advantages, there are, however, many disadvantages. In practice, the following factors have a great influence on finding a peak of cross-correlation function. The correlation is essentially the square of the signal, so within any volume the largest signal changes, and hence the largest flow structures, dominate the result.

The time window must be determined in such a way that correlation function calculated of the flow pattern over the window contains an evident peak.

Figure 1a shows the typical concentration changes within a chosen pixel for the two planes as the function of a frame number and figure 1b shows a graph of the corresponding correlation function. As can be seen, the calculated function has no evident peak, and thus using one to determine the transit time is not easy. Hence, classical methods calculating a flow velocity based on the correlation of the corresponding pixels are not suitable for certain flow-patterns and finding the peak of a correlogram is ambiguous.

These limitations seriously restrict the application of cross-correlation in flow measurement and the range of operating conditions where reliable answers can be obtained. The weighted-mean phases method (Mosorov 2006) overcomes these limitations permitting the flow velocity to be unambiguously calculated with high robust. It is based on a spectrum analysis of the pixel values of both cross-sections of the tomographic system.

In the case of the weighted-mean phases method, a transit time τx is calculated as the weighted-mean value of the time translations τk of the same k-harmonics of xn and yn signals:

$$\tau_x = \sum_{k=1}^{K}\left[(A_k^x + A_k^y)/\sum_{k=1}^{K}(A_k^x + A_k^y)\right]\cdot\frac{1}{k\cdot\omega_0}(\varphi_k^x - \varphi_k^y) \qquad (3)$$

where Akx and Akx are the amplitudes and φkx and φky are the phases of the kth spectral components Sxn(jkω0), Syn(jkω0) of the xn and yn respectively.

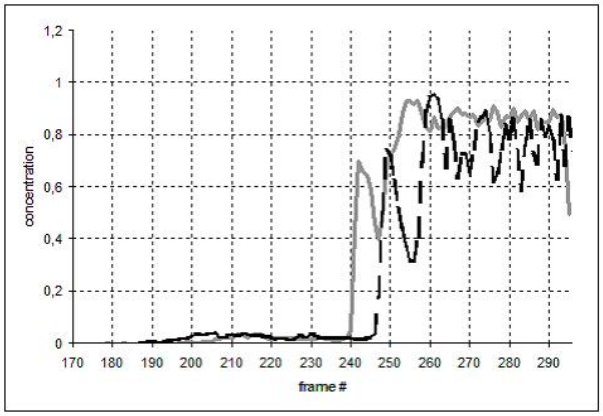

a)

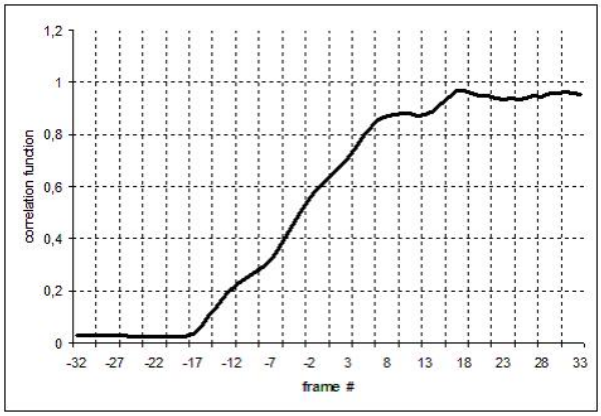

b)

Fig. 1. Solid concentration changes within chosen pixel:(a) light grey line is 1 plane concentration, dashed black line is 2 plane concentration (b) calculated correlation function for the time window 64 frames

The proposed method can easily be applied to the existing flowmeters based on twin plane tomographic system by upgrading the software. The one has no

limitation on the application for other types of modality such as gamma or optical tomography.

The aim of the paper is to evaluate the robust of the weighted-mean phases method and its applicability to calculate a flow velocity using by a twin-plane electrical tomography system.

3. Method study

All experiments described in this paper were carried out for simple gravity-drop flow using the twin-plane ECT system. The rig schematic and dimensions of the sensor planes installation are shown in Figure 2. The measured volume (pipe fragment with an inner diameter of around 5 cm) was filled with plastic beads.

The beads are retained by a valve above two sensor planes consisting of 8 electrodes connected to a ECT system. The distance between the sensor plane centres was d=90 mm. The first sensor plane was located approximately 320 mm below the neck of the hopper funnel.

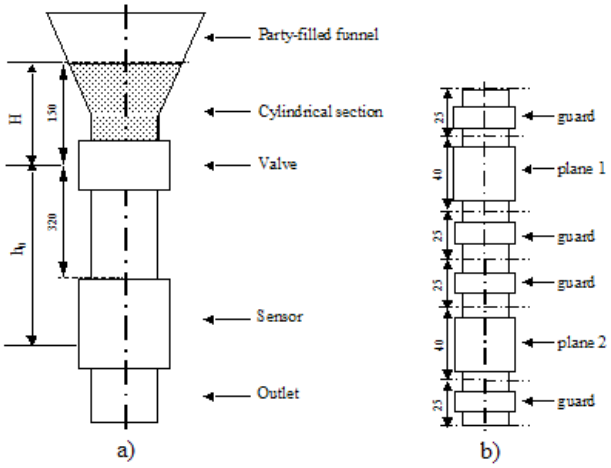

Fig. 2. (a) gravity drop rig schematic (b) sensor configuration

The ECT system had been calibrated by successively filling with air and then beads to give a concentration range from 0 to 1. The modified Landweber iteration algorithm (Yang et al 1999) is used for image reconstruction. Each image comprises 32x32 pixels so that the total pixel number N was equal to 1024.

We are going to open the valve and then the plug, which appears under gravity and passes from the funnel through the pipe, can be used to measure the transit time using both classic cross-correlation method and the proposed method. The typical time of plug propagation was less then 1 sec.

Figure 3a, shows the concentration changes for the central pixel of the cross-section as the function of a frame number for two typical tests with data acquisition of 100 frames per second of two sensor planes.

It can be seen from these graphs that after the valve is opened, a dense plug of pellets falls between about the 530th frame and 620th frame (figure 3a). The transit time between the front edges of the 'spike' of the concentration of the upper and lower plane corresponds to around 3 frames within the frame rate resolution of 0.01s.

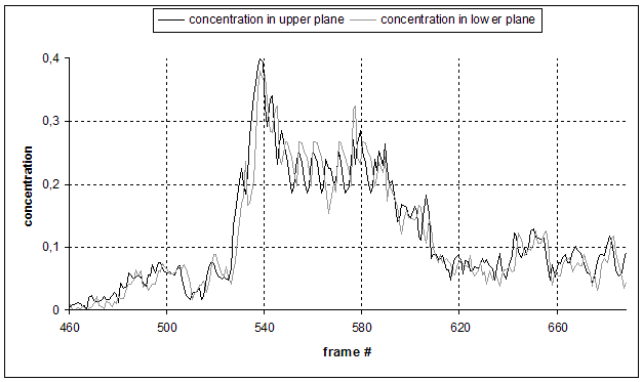

a)

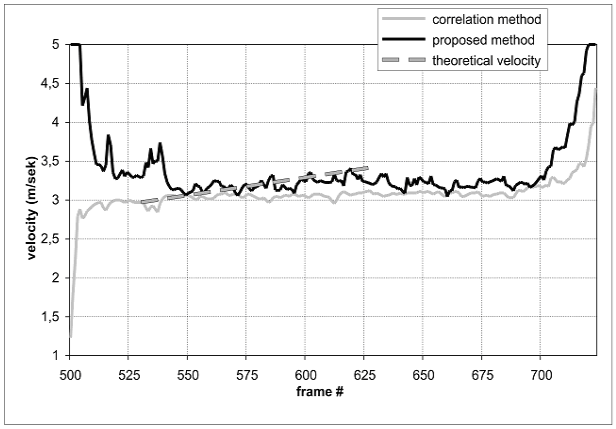

b)

Fig. 3. (a) Graph of concentration against time for gravity drop flow in central pixel (b) graph of velocity against time for gravity drop flow (a) calculated by proposed method and correlation method

A theoretical plug velocity vx of pellets falling from a height h_x (without air resistance) can be evaluated as follows:

$$v_x = \sqrt{2 \cdot g \cdot h_x} \tag{4}$$

where g is the acceleration of free fall (9.81 m/sec^{-2}).

Assuming that h_x=h_0+Δh_x, 0≤Δh_x≤H, where h_0 is the distance from the valve to the lower plane, and H is the height of the pellets partially filling the funnel (see figure 3a), the velocity for any time during a plug on the lower plane level can then be calculated as:

$$v_x = \sqrt{2 \cdot g \cdot (h_0 + \Delta h_x)} = \sqrt{2 \cdot g \cdot (h_0 + \Delta t_x \cdot v_0 + (g \cdot \Delta t_x{}^2)/2)} \tag{5}$$

where $v_0 = \sqrt{2 \cdot g \cdot h_0}$, $\Delta t_x = t_x - t_b$ is the difference between time t_x and time t_b, when a plug reaches the lower plane calculated as

$$t_x = \sqrt{2 \cdot (h_0 + \Delta h_x) \cdot g^{-1}}, \qquad t_b = \sqrt{2 \cdot h_0 \cdot g^{-1}}.$$

According to (5) the beginning velocity of the plug is 2.97 m/sec and terminal velocity is 3.43 m/sec. The

speed is not the same because the lowest pellets fall about h_0=45 cm before arriving at the lower plane of the sensor, while the upper pellets fall about h_0+H=60 cm.

An example of transit time calculation for frame #620 by the proposed method is presented in table 1. The total number of pixel values for which the DFT transformations are calculated K is equal to 14. It is observable that the transit time value by the proposed method (τ=2.6479 frames) corresponds well to the theoretical transit time 2.6231 frames.

Figure 3b shows the changes of solid velocity derived from both the correlation and phase method discussed above versus time during a gravity drop flow (see figure 3a). In the case of the correlation method, the peaks were found by the polynomial fitting method, and determining peaks (during plug motion only) was sufficiently simple.

Since the given velocities of both methods are calculated at time window (140 frames) they are not temporary velocities. Therefore there exists a continuation of the velocity graph after the plug body propagation (the velocity graph at #630-700 frames in figure 3b).

As it can be seen, the velocities calculated from both methods are almost the same, although velocity calculated by the proposed method is a little more accurate compared with theoretical velocity (around 5%) than one calculated by the correlation method.

The probable reason that the phase method gives better results than the correlation method is that correlation is essentially the square of the signal and hence the largest signal changes dominate the result; therefore the dispersion of these calculated values is small. Otherwise the phase method is more sensitive even for smaller signal changes. This is probably also the reason that the dispersion of velocity values by the proposed method is higher in comparison with those derived by the correlation method.

It is obvious that the proposed method can only be used when there exists a correlation between measured values from the two planes, i.e. material motion between two planes. Thus in our experiments outside of plug propagation, the proposed method cannot be applied because there doest not exist a relationship between signals of the two planes.

4. Conclusion

A weighted-mean phases method permitting a time-delay between two signals to be calculated with higher accuracy is studied. This is based on an analysis of differences between phases of the same harmonics of the received signals. Contrary to the methods using a cross correlation function, which need some limits regarding a form of a correlation function, such as one extremum presence, this method is more applicable. The results using the pneumatic conveying flow show that the proposed estimator achieves a bit more accuracy. Finally, the proposed estimator is relatively fast in software implementation because two independent FFT transformations are needed instead of correlation function calculation.

Table 1. An example of transit time calculation for frame #660 by the proposed method (eq. 3)

k,	Phase φ^x_k (radian)	Phase φ^y_k (radian)	φ^x_k,- φ^y_k, (radian)	τ_k (frame)	Weight w_k,
1	-1.4471	-1.5454	0.0983	3.9118	0.2427
2	-2.8780	-3.0459	0.1679	3.3399	0.2209
3	2.1824	1.9621	0.2203	2.9221	0.1397
4	1.0968	0.8481	0.2487	2.4742	0.0926
5	-0.6797	-1.0552	0.3755	2.9884	0.0411
6	2.6630	2.3915	0.2715	1.8005	0.0458
7	1.4789	0.9857	0.4931	2.8030	0.0372
8	-0.1794	-0.2803	0.1009	0.5019	0.0105
9	2.5989	2.1001	0.4987	2.2049	0.0490
10	1.5180	1.4257	0.0923	0.3674	0.0101
11	1.0512	0.5492	0.5020	1.8158	0.0388
12	-0.6567	-1.4175	0.7607	2.5224	0.0282
13	2.6333	2.2536	0.3797	1.1621	0.0275
14	2.3225	1.6545	0.6679	1.8983	0.0160

τ≈2.9550 frames

REFERENCE

BECK M.S., (1981), Correlation in instruments: cross correlation flowmeters, *Journal of Physics E: Scientific Instruments*, Vol. 14 , pp. 7-19.

BOLTON G. T., HOOPER C. W., MANN R., STITT E.H., (2003) Flow distribution and velocity in a radial flow fixed bed reactor using electrical resistance tomography, 3rd World Congress on Industrial Process Tomography, Banff, Canada, pp 813-820.

BYARS M., PENDLETON J. D., GOODEVE D., (2003) A New High-Speed Control Interface for an Electrical Capacitance Tomography System, 3rd World Congress on Industrial Process Tomography, Banff, Canada, pp. 631-636.

CORLETT A. E., (2001) Determination of Flow Patterns and Void Fraction of Multiphase Flows Using Electrical Capacitance Tomography. 2nd World Congress on Industrial Process Tomography, Hannover, Germany, p.636-643.

FEHMERS G., (2003) Volumetric flow rates from impedance tomography in oil/gas flown. 3rd World Congress on Industrial Process Tomography, Banff, Canada, pp. 287-292.

HUNT A., PENDLETON J. D., WHITE R. B, (2003) A Novel Tomographic Flow Analysis System. 3rd World Congress on Industrial Process Tomography, Banff, Canada, pp. 281-286.

JAWORSKI A., DYAKOWSKI T., (2001), Tomographic measurements of solids mass flow in dense pneumatic conveying. What do we need to know about the flow physics? 2nd World Congress on Industrial Process Tomography, Hannover, pp. 353-360.

MOSOROV V., (2006), A method of transit time measurement using twin plane electrical tomography, *Measurement Science and Technology*, Vol. 17, pp 753-760.

MOSOROV V., SANKOWSKI D., MAZURKIEWICZ L., DYAKOWSKI T., (2002), The 'best-correlated pixels' method for solid mass flow measurement using electrical capacitance tomography. *Measurement Science and Technology,* Vol. 13, pp. 1810-1814.

WILLIAMS R. A., BECK M. S., (1995), *Process Tomography: Principles, Techniques and Applications*. Oxford: Butterworth-Heinemann.

YANG W. Q. SPINK D.M., YORK T.A., MCCANN H., (1999), An image-reconstruction algorithm based on Landweber's iteration method for electrical-capacitance tomography. *Measurement Science and Technology*, Vol. 10, pp. 1065-1069.